Citation for published version:
Pei, X, Zeng, X, Smith, AC & Malkin, D 2015, 'Resistive superconducting fault current limiter coil design using multistrand MgB2 wire', *IEEE Transactions on Applied Superconductivity*, vol. 25, no. 3, 7006791. https://doi.org/10.1109/TASC.2015.2390635

DOI:
10.1109/TASC.2015.2390635

Publication date:
2015

Document Version
Peer reviewed version

Link to publication

Resistive Superconducting Fault Current Limiter Coil Design using Multi-strand MgB_2 Wire

Xiaoze Pei, Xianwu Zeng, Alexander C. Smith, *Senior Member IEEE*, and Daniel Malkin

***Abstract*—Resistive superconducting fault current limiters (SFCLs) offer the advantages of low weight and compact structure. Magnesium Diboride (MgB_2) in simple round wire form has been tested previously and shown to be suitable as a low-cost resistive SFCL. The primary objective of this work was to design a resistive SFCL for an 11kV substation using multiple MgB_2 wire strands. The paper will look into the options for the coil design. Two types of low inductance solenoidal coils: the series connected coil and the parallel connected coil were theoretically examined and compared. This paper also reports the experimental results of two multiple strand MgB_2 prototype coils used as a resistive SFCL. This paper demonstrates the potential of SFCL coils using multi-strand MgB_2 wire for distribution network levels.**

***Index Terms*—Multi-strand, MgB_2, Low inductance coil, Superconducting fault current limiter, SFCL**

I. Introduction

Superconducting fault current limiters (SFCLs) are an alternative option for upgrading the transformerS and circuit breakers in land-based power networks because fault current levels are generally rising in many distribution systems, commonly with the addition of renewable generation. Resistive SFCLs offer the advantages of low weight and compact structure [1]. Magnesium Diboride (MgB_2), which was found to exhibit superconductivity below 39 K in 2001 [2], currently can be manufactured in various forms: round wire; rectangular wire or flat tape [3-5]. MgB_2 in simple round wire form has been tested previously and shown to be suitable for low-cost resistive SFCLs [6-8]. The primary objective of this work was to design a resistive SFCL for an 11kV substation using multiple MgB_2 wire strands. The load current under normal operating conditions was 1250 Arms, which meant it was unlikely that a single MgB_2 wire would be feasible. Multiple MgB_2 wire strands were used to increase the current capacity. One of the key performance aspects was ensuring that each wire strand carries the same current. Any non-uniform current distribution effectively reduces the overall current capacity of the multi-strand wire. Multiple wire strands were therefore transposed into a braid or rope configuration to equalize the impedance of each parallel wire path [7]. Minimum coil inductance is another important criterion for an SFCL coil design. This is traditionally achieved by means of a pancake type non-inductive coil using a bifilar winding arrangement. However, this winding arrangement leads to cooling issues as the coil turns in the center are not fully exposed to the coolant [9, 10]. This paper will examine the alternative options for the coil design.

The paper compares two solenoidal type bifilar coil topologies: a series connected coil and a parallel connected coil. Both of them are made with two windings connected to cancel the main magnetic field produced by each other so that a low inductance is achieved [11, 12].

Multiple MgB_2 wire strands were used to build the series and parallel connected SFCL prototype coils. This paper reports on the experimental results of these two coils used as a resistive SFCL. The paper also includes a detailed analysis of the results and the implications for the practical design of commercial SFCLs.

II. Coil Design

During normal operation, it is necessary to keep the inductance of the SFCL coil as low as possible so that the effect on the networks is minimized. Pancake type non-inductive bifilar coil is an obvious option. However, this coil suffers from excessive joule heating during a quench and has the disadvantage of a long recovery time after a fault due to the way the coil is stacked together. Two alternative solenoidal coil arrangements: the series connected coils and the parallel connected coils are shown in Fig. 1. Both coils are made of two windings with the second winding cancels the magnetic field produced by the first one providing a minimum inductance.

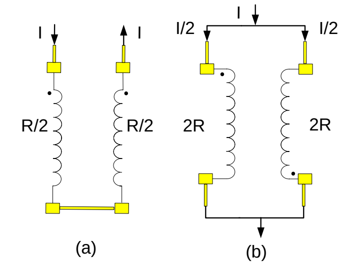

Fig. 1. SFCL coil topology: (a) series coil; (b) parallel coil

Manuscript received August 11, 2014. This work was funded by Energy Technologies Institute (ETI). The authors would like to thank Energy Technologies Institute, Rolls-Royce Plc, Applied Superconductor Limited (ASL) and Hyper Tech Research, Inc.

The authors are with the School of Electrical and Electronic Engineering, The University of Manchester, Manchester, M13 9PL UK. (phone: +44-161-306-4667; fax: +44-161-306-4774; e-mails: xiaoze.pei@manchester.ac.uk, sandy.smith@manchester.ac.uk).

These two coil topologies both have to be designed to the same specification to operate at the same current to enable the coil to be compared with each other. The operating current of the SFCL is assumed to be I_o and the minimum quench resistance during a fault is R_f. The same superconducting wire type is used in the design for comparison purposes. Let us suppose the cross-sectional area of the superconducting material is A, the wire critical current is I_c, and the quench resistance per unit length of the wire is R_q. It is also assumed here that the wire operates at 60% of its critical current under normal operating conditions.

The number of wire strands required for the series coil in Fig. 1(a) is:

$$N_{series} = \frac{I_o}{0.6 I_c} \quad (1)$$

The length of each winding is:

$$l_{series} = \frac{R_f / 2}{R_q / N_{series}} = \frac{R_f N_{series}}{2 R_q} \quad (2)$$

The total length of the wire used is thus:

$$l_{series}^{wire} = N_{series} \times l_{series} \times 2 = (\frac{I_o}{0.6 I_c})^2 \frac{R_f}{R_q} \quad (3)$$

The volume of the superconducting material in the series coil is:

$$V_{series} = l_{series}^{wire} \times A = (\frac{I_o}{0.6 I_c})^2 \frac{R_f A}{R_q} \quad (4)$$

The number of wire strands of each winding for the parallel coil is half of the series coil:

$$N_{parallel} = \frac{I_o / 2}{0.6 I_c} = \frac{I_o}{1.2 I_c} = \frac{N_{series}}{2} \quad (5)$$

The resistance of each winding after quench should be $2R_f$ as the two windings are connected in parallel. The length of each winding is:

$$l_{parallel} = \frac{2R_f}{R_q / N_{parallel}} = 2 l_{series} \quad (6)$$

The length of the wire used for the parallel winding is:

$$l_{parallel}^{wire} = N_{parallel} \times l_{parallel} \times 2 = (\frac{I_o}{0.6 I_c})^2 \frac{R_f}{R_q} = l_{series}^{wire} \quad (7)$$

The volume of superconducting material in the parallel winding therefore is,

$$V_{parallel} = l_{parallel}^{wire} \times A = (\frac{I_o}{0.6 I_c})^2 \frac{R_f A}{R_q} = V_{series} \quad (8)$$

It is clear that each winding in the parallel connection has half the area and twice the length compared with the series connection. If the same wire size is used in both connections, the series connection would require twice the number of wire strands in each coil as the parallel connection, and the net length of wire needed in both connections is the same. The total volume of superconducting material is the same for any given design specification.

The AC losses under normal operation are an important factor in the design of the SFCL coil. The Norris model can be used to estimate the hysteresis losses in type II superconductors [13]. The hysteresis loss per cycle per unit length in a round wire is:

$$L_c = I_c^2 \mu_0 L_1(F) \quad (9)$$

where L_1 is given as a function of F and F is the ratio of the transport current to the critical current [13].

The AC losses of the SFCL coil can be expressed as:

$$P = L_c \times f \times l^{wire} \quad (10)$$

where f is frequency of the power networks and l^{wire} is the length of the wire used in the SFCL coil.

If both the series and parallel coils use the same wire strand size and F is 0.6, each wire strand per unit length for these two coils would have the same AC losses. The total length of the wire used in these two coils has been proved to be the same; the total AC losses therefore would be the same if the proximity effect is not considered. It should be pointed out that this conclusion assumes the same wire size is used.

Voltage insulation in the two coil connections also requires design consideration. The worst case fault scenario would result in full voltage appearing across the input and output terminals of the SFCL. In the series connection, the input and output connections are both at one end of the coil unit and adjacent turns at this end see full voltage across them. The voltage across adjacent turns reduces linearly to nearly zero at the coil unit end opposite the terminals. In the parallel connections, the voltage across adjacent turns is constant from the end to the other of the coil unit. The insulation system needs to take these different voltage gradients along the coils into account. Grading the separation distances in the series connection can be used to reduce the overall size of the coil unit so that is closely similar to that of the parallel connection.

III. Experimental Setup

A. SFCL Prototype Coils

A monocore MgB_2 wire using a stainless steel sheath manufactured by Hyper Tech Research, Inc. was used for the prototype coils. The diameter of each individual wire was 0.36 mm and the DC critical current was approximately 23.4 A at 25 K. Stainless steel was selected as the sheath material to provide a high resistance per unit length. Current sharing in each wire strand is a critical factor for an SFCL coil using multiple strands. In practice, there have been quite a lot of problems in ensuring uniform distribution of the current [14]. To ensure uniform current in each wire strand, the wire strands were transposed into a braid configuration to equalize the impedance of each parallel wire path.

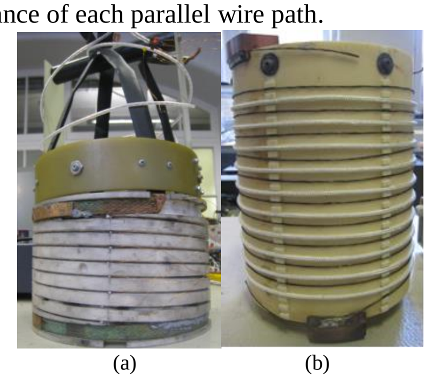

(a) (b)

Fig. 2. SFCL prototype coils: (a) series coil; (b) parallel coil

Fig. 2 shows the two prototype SFCL coils. The diameter of the alumina former was 200 mm. (a) is the series connected coil: each winding was made of three MgB_2 wire strands with three and half turns. The input and output current terminals were situated at the top of the alumina former. (b) is the parallel connected coil: each winding was made of seven strand MgB_2 wire strands and had ten and three quarters turns. The inner winding was wound clockwise on the former. The outer winding was sheathed with S-glass insulation and then wound counterclockwise. The input and output current terminals in this were situated at opposite ends of the former.

B. Test Circuit

The operation of these two SFCL coils was tested using a controllable high current supply, which is shown in Fig. 3 [7]. A variac was manually adjusted to simulate different potential fault current levels. Voltage, current and temperature signals were recorded using a PC based LabVIEW system. The number of AC cycles supplied to the test coil was also controlled by the LabVIEW system.

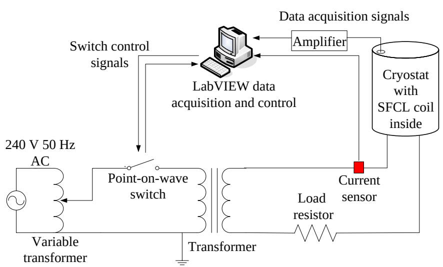

Fig. 3. High current test circuit schematic

The AC loss measurement circuit is shown in Fig. 4. A 50 Hz sinusoidal signal was generated using the network analyzer and then amplified using a power amplifier. In order to increase the current level, a voltage step-down transformer was also used. The voltage and current signals were measured by the network analyzer and precision oscilloscope.

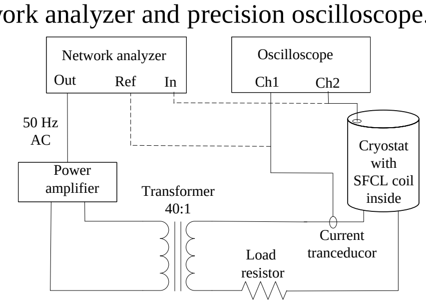

Fig. 4. AC loss measurement circuit schematic

IV. Experimental Results and Discussion

A. Quench Current

The high current test circuit was used to pass two cycles of high current through the SFCL coil. The potential peak current level was gradually increased by adjusting the set point of the variac. The potential peak current was calculated based on the coil in the superconducting state with negligible impedance.

The three-strand series coil with a wire diameter of 0.36 mm shown in fig. 2(a) was tested. Fig. 5 shows the quench response during a short cycle test at 25 K with a potential peak current of 200 A. Voltage channel 1 measures the voltage across the first winding whilst voltage channel 2 measures the voltage across the second winding. The voltage signal is clamped because of the LabVIEW input voltage limitation. It is obvious that the two windings do not quench at the same current level. The first winding quenches (or a section of it) whilst the second winding is still in the superconducting state. This is thought to be due to the critical current variation along the wire created during the wire manufacture.

Seven-strand parallel coil as shown in fig. 2(b) was then tested. Figures 6 to 9 show the quench response of the parallel coil during the short cycle test at 25 K with a potential peak current of 600 A. Voltage channel 1 measures the voltage across the inner winding whilst voltage channel 2 measures the voltage across the outer winding. Figures 7 and 9 clearly show that the inner winding quenches at 6.5 milliseconds and drives the current into the outer winding. This imbalanced current sharing develops a solenoidal magnetic field. The resulting high current in the outer winding causes it to start to quench at 8 milliseconds. The current then transfers back and equalizes the currents in the two coils, cancelling the solenoidal field again. This current transfer mechanism ensures a rapid quench once the onset of quench occurs.

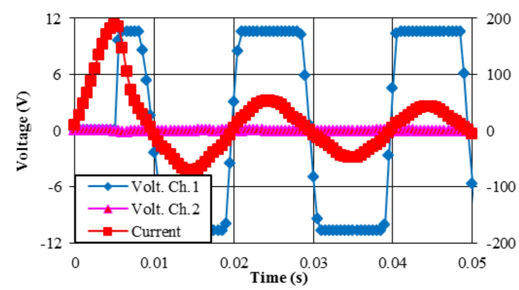

Fig. 5. Quench response of the series coil at 25 K with a potential peak current of 200 A

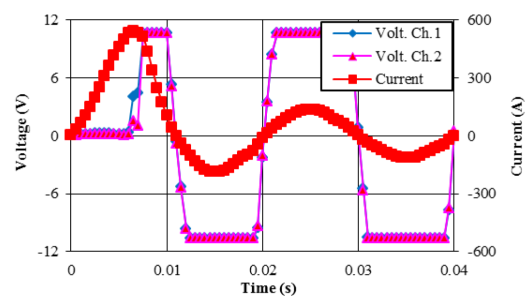

Fig. 6. Quench response of the parallel coil at 25 K with a potential peak current of 600 A

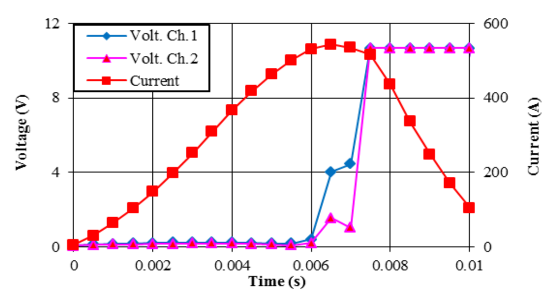

Fig. 7. Quench response of the parallel coil at 25 K with a potential peak current of 600 A, highlighting the quench point

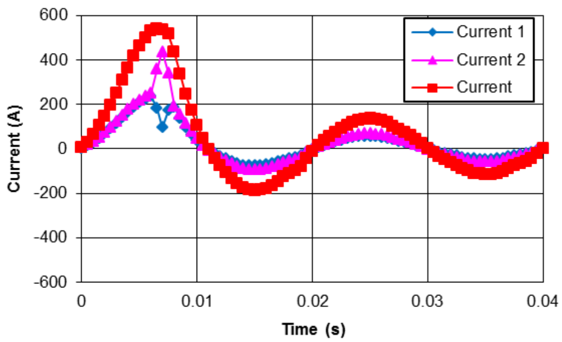

Fig. 8. Current sharing of the parallel coil at 25 K with a potential peak current of 600 A

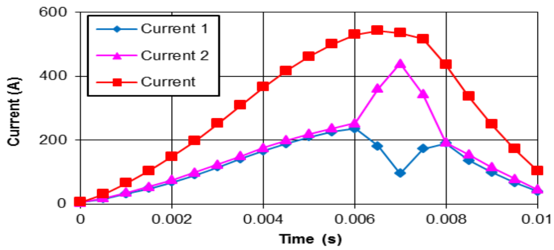

Fig. 9. Current sharing of the parallel coil at 25 K with a potential peak current of 600 A, highlighting the quench point

The quench current of both coils was measured from 32 K to 25 K. The quench current density shown in Fig. 10 was calculated using the quench current and the area of the MgB_2 core. The quench current density of both coils increases approximately linear as temperature reduces as expected. The DC critical current density is 750 A/mm^2 at 25 K and the AC quench current density is expected to be 2-3 times the DC critical current density [15]. The quench current density of the three-strand series connected coil is 2.68 times the DC critical current density at 25 K. The quench current density of the seven-strand parallel connected coil however is only 1.52 times the DC critical current density, which is not as good as expected. Fig. 10 also shows that the quench current density of the seven-strand parallel connected coil is not as good as the three-strand series connected coil. It is believed that this could be related to the number of wire strands of each coil instead of the winding topologies. There are two possible reasons which may explain this: firstly, the current distribution in the seven-strand coil is less uniformly distributed compared with the three-strand coil due to differences in the proximity effect; secondly, the reduced quench current density could be related to the double twisting process used to fabricate the seven-strand winding putting additional stresses on the wire.

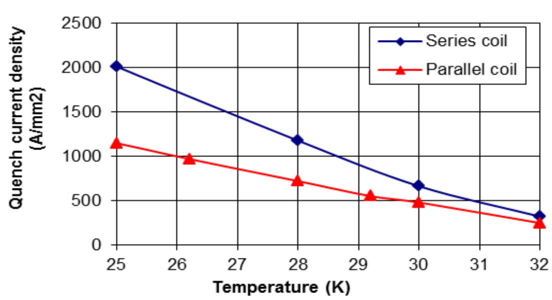

Fig. 10. Quench current density versus temperature (self-field)

B. *AC Losses*

The instantaneous current and voltage signals from the SFCL coil were measured using a high sampling rate oscilloscope. The instantaneous current was then multiplied by the instantaneous voltage to acquire the instantaneous power. The instantaneous power was then integrated over a cycle to obtain the real power, corresponding to the AC losses [16]. The AC losses of the series and parallel connected coils are shown in Fig. 11. It is clear from the trend line that the AC losses closely follow a current squared dependence. This may indicate that the measured losses are dominated by the eddy current losses in the cryostat copper container. The losses in the series coil are slightly higher than in the parallel coil. This is because each strand of the series coil is carrying higher current than the parallel coil, which would have higher hysteresis losses according to the Norris model.

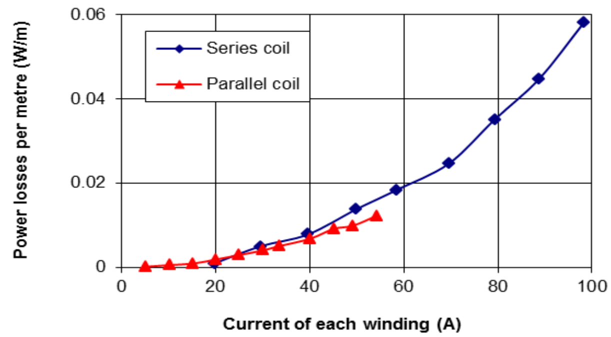

Fig. 11. AC losses comparison

V. Conclusion

In this paper, two solenoidal type bifilar coils were proposed as a resistive SFCL coil design. The series connected coil ensures equal current in both windings naturally. The parallel coil has certain beneficial features for high voltage applications. It has been theoretically proved that both coils use the same amount of material and have the same AC losses under the same design specification using the same superconducting wire size.

Two prototype coils, one series and one parallel connected coil, were built and tested. Both coils demonstrated repeatable and reliable operation as a resistive SFCL. The quench mechanism of the parallel coil ensures a rapid, current-transfer triggered quench once the onset of quench occurs.

This paper also demonstrates the potential of designing SFCL coils using multi-strand MgB_2 wire for distribution network levels.

Acknowledgment

This work was funded by Energy Technologies Institute (ETI). The authors would like to thank Energy Technologies Institute, Rolls-Royce Plc, Applied Superconductor Limited (ASL) and Hyper Tech Research, Inc.

References

[1] M. Noe, and M. Steurer, "High-temperature superconductor fault current limiter: concept, application, and development status," *Supercond. Sci. and Technol.*, vol. 20, pp. R15-R29, Mar. 2007.

[2] J. Nagamatsu, N. Nakagawa, T. Muranaka, Y. Zenitani, J. Akimitsu, "Superconductivity at 39 K in magnesium diboride", *Nature*, 410, pp. 63-65, 2001.
[3] M. Tomsic, M. Rindfleisch, J. Yue, K. McFadden, D. Doll, J. Phillips, M. D. Sumption, M. Bhatia, S. Bohnenstiehl, and E. W. Collings, "Development of Magnesium Diboride (MgB_2) Wires and Magnets using in situ Strand Fabrication Method," *Physica C: Superconductivity*, vol. 456, pp. 203-208, Jun. 2007.
[4] G. Z. Li, Y. Yang, M. A. Susner, M. D. Sumption, and E. W. Collings, "Critical current densities and n-values of MgB_2 strands over a wide range of temperatures and fields," *Supercond. Sci. and Technol.*, vol. 25, 025001, Feb. 2012.
[5] J. Pelegrín, G. Romano, E. Martínez, L. A. Angurel, R. Navarro, C. Ferdeghini, S. Brisigotti, G. Grasso, and D. Nardelli, "Experimental and numerical analysis of quench propagation on MgB_2 tapes and pancake coils," *Supercond. Sci. and Technol.*, vol. 26, 045002, Apr. 2013.
[6] A. Oliver, A. C. Smith, M. Husband, M. Bailey, and Y. Feng, "Assessment of small bend diameter magnesium diboride wire for a superconducting fault current limiter application," *IEEE Trans. Appl. Supercond.*, vol. 19, pp. 1942-1945, Jun. 2009.
[7] X. Pei, A. C. Smith, M. Husband, and M. Rindfleisch "Experimental tests on a superconducting fault current limiter using three-strand MgB_2 wire," *IEEE Trans. Appl. Supercond.*, vol. 22, 5600405, Jun. 2012.
[8] A. C. Smith, A. Oliver, X. Pei, M. Husband, and M. Rindfleisch, "Experimental testing and modelling of a resistive type superconducting fault current limiter using MgB_2 wire," *Supercond. Sci. and Technol.*, vol. 25, 125018, Dec. 2012.
[9] M. C. Ahn, D. K. Bae, S. E. Yang, D. K. Park, T. K. Ko, B.-Y. Seok, C. Lee, and H.-M. Chang, "Manufacture and test of small-scale superconducting fault current limiter by using the bifilar winding of coated conductor," *IEEE Trans. Appl. Supercond.*, vol. 16, pp. 646–649, June 2006.
[10] D. K. Park, M. C. Ahn, S. Park, H. Kang, D. K. Bae, S. E. Yang, B.-Y. Seok, and T. K. Ko, "An analysis and short circuit test of various types of Bi-2223 bifilar winding fault current limiting module," *IEEE Trans. Appl. Supercond.*, vol. 16, no. 2, pp. 703–706, June 2006.
[11] C. Lee, H. Kang, M. C. Ahn, T. K. Ko, and B.-Y. Seok, "Short-circuit test of novel solenoid type high-Tc superconducting fault current limiter," *Cryogenics*, vol. 47, pp. 380-386, April. 2007.
[12] B.-Y. Seok, H. Kang, C. Lee, K. Nam, Y. Kim, and T. K. Ko, "Electrical insulation design of 13.2 kV/630 A bifilar winding type HTS fault current limiter," *IEEE Trans. Appl. Supercond.*, vol. 17, pp. 1505-1508, June 2007.
[13] W. T. Norris, "Calculation of hystersis losses in hard superconductors carrying ac: isolated conductors and edges of thin sheets," *J. Phys. D: Appl. Phys.*, vol. 3, pp. 489-507, Apr. 1970.
[14] K. Shimohata, S. Yokoyama, T. Inaguchi, S. Nakamura and Y. Ozawa, "Current distribution measurement in YBCO thin film for a superconducting fault current limiter", *Cryogenics*, vol. 43, pp. 111-116, Feb. 2003.
[15] L. Ye, M. Majoros, A. M. Campbell, T. A. Coombs, S. Harrison, P. Sargent, M. Haslett and M. Husband, "Investigations of current limiting properties of the MgB_2 wires subjected to pulse overcurrents in the benchtop tester," *Supercond. Sci. and Technol.*, vol. 20, pp. 320-326, April 2007.
[16] John H. Scofield, "A frequency-domain description of a lock-in amplifier," *Ame. J. of Phys.*, vol. 62, pp. 129-133, Feb. 1994.